R. & M. No. 3091
(19,056)
A.R.C. Technical Report

MINISTRY OF SUPPLY

AERONAUTICAL RESEARCH COUNCIL
REPORTS AND MEMORANDA

An Experimental Investigation of Leading-Edge Flow Separation from a 4 per cent Thick Two-Dimensional Biconvex Aerofoil

By

B. D. HENSHALL, B.Sc., PH.D.,
and R. F. CASH, A.F.R.AE.S. of the Aerodynamics Division, N.P.L.

LONDON : HER MAJESTY'S STATIONERY OFFICE
1958
PRICE 6*s.* 6*d.* NET

An Experimental Investigation of Leading-Edge Flow Separation from a 4 per cent Thick Two-Dimensional Biconvex Aerofoil

By

B. D. HENSHALL, B.Sc., PH.D.,
and R. F. CASH, A.F.R.AE.S. of the Aerodynamics Division, N.P.L.

Reports and Memoranda No. 3091*

February, 1957

Summary.—The development of leading-edge flow separation as incidence is raised, for a 4 per cent thick two-dimensional biconvex aerofoil, was studied experimentally for wide ranges of incidence at Mach numbers of 0·40, 0·50, 0·60 and 0·70. Pressure distributions and flow photographs are presented which illustrate the growth of the ' bubble ' of separated flow.

1. *Introduction.*—Current tests in the high-speed wind tunnels at the National Physical Laboratory on two-dimensional aerofoils are made over wide ranges of incidence and Mach number from low subsonic ($M_0 \simeq 0{\cdot}40$) to moderate supersonic ($M_0 = 1{\cdot}60$) speeds. In these investigations the main emphasis is placed on a study of the boundary-layer separations which occur during various phases of the incidence and speed ranges considered. These boundary-layer separations are usually classified into three types: the leading-edge separation[1] which occurs as the incidence is increased at a fixed Mach number which is low enough for the flow to be essentially similar to that studied in low-speed wind tunnels; the shock-induced separation[2] which occurs on aerofoils at high subsonic and transonic speeds and the trailing-edge shock-induced separation[3] which occurs on aerofoils at incidence at supersonic speeds. Although the two latter types are particular cases of the general interaction between shock waves and boundary layers[4], it is convenient to classify them separately.

One such general investigation of the types of boundary-layer separation has been made with a 4 per cent thick two-dimensional biconvex aerofoil in the 36-in. × 14-in. High-Speed Wind Tunnel. This report presents the results for the leading-edge type of boundary-layer separation at low speeds; subsequent reports will describe the transonic and supersonic characteristics of this aerofoil.

2. *Experimental Data.*—Tests on a 4 per cent thick biconvex aerofoil of 9-in. chord and 14-in. span have been made in the 36-in. × 14-in. High-Speed Wind Tunnel at the N.P.L. A selection of surface-pressure distributions and schlieren photographs for wide ranges of incidence at Mach numbers of 0·40, 0·50, 0·60, and 0·70 appear as Figs. 1 to 8. The Reynolds numbers of the tests vary from $1{\cdot}9 \times 10^6$ at $M_0 = 0{\cdot}40$ to $2{\cdot}9 \times 10^6$ at $M_0 = 0{\cdot}70$. Two series of preliminary experiments were made, with and without layers of carborundum, approximately five-thousandths of an inch thick, on the first 0·05 chord of both surfaces of the aerofoil. When the corresponding surface-pressure distributions and photographs from the two series were compared, the results were found to be identical within the limits of experimental errors. Transition always occurred under the adverse pressure gradient immediately downstream of the nose as soon as incidence was applied to the model. Hence all the subsequent tests reported below were conducted without the use of artificial transition methods.

* Published with permission of the Director, National Physical Laboratory.

From the surface-pressure distributions the normal-force coefficients were calculated by integration and these results are presented in Fig. 9. It may be noted that the ratio of the normal-force curve slopes, *viz.*,

$$\left(\frac{dC_N}{d\alpha}\right)_{M_0=0\cdot70} \Big/ \left(\frac{dC_N}{d\alpha}\right)_{M_0=0\cdot40}$$

is 1·26 compared with the Prandtl-Glauert theoretical value of 1·28.

3. *Analysis and Discussion of Results.*—In this investigation the emphasis has been placed on the occurrence and subsequent growth of the bubble of separated flow on the upper surface of the aerofoil. The above pressure distributions have therefore been analysed in various ways in order to illustrate those features of the general flow which are relevant to bubble occurrence and growth.

For any aerofoil, the variation of the trailing-edge pressure is intimately related to the development of the flow around the whole aerofoil. Furthermore, it has been established that the onset of the effects of separation is marked by a divergence of trailing-edge pressure from its normal smooth variation. Curves of trailing-edge pressure ratio $(p/H_0)_{TE}$ plotted against incidence α for various free-stream Mach numbers M_0 are presented in Fig. 10, where the deviations from linear variation of $(p/H_0)_{TE}$ with α are indicated.

The variation of the pressure in the bubble is conveniently shown in Fig. 11 by a plot of pressure ratio at 0·05 chord against incidence for several free-stream Mach numbers M_0. After a small bubble of separated flow is formed on the upper surface of the aerofoil and the bubble continues to grow in chordwise extent as the incidence is increased, it may be noted that the pressure in the bubble remains approximately constant until the effects of the separation reach the trailing edge of the aerofoil. Thereafter the bubble pressure ratio $(p/H_0)_{0\cdot05c}$ increases and the trailing-edge pressure ratio $(p/H_0)_{TE}$ decreases until their values coincide when the bubble has extended over the whole of the upper surface of the aerofoil. Fig. 12 illustrates this variation of $(p/H_0)_{TE}$ with $(p/H_0)_{0\cdot05c}$ as the incidence is raised at several fixed Mach numbers. The same data are plotted more clearly in Fig. 13 by the use of the parameter $(p_0 - p_{TE})/H_0$ instead of $(p/H_0)_{TE}$ as ordinate.

A general qualitative discussion of the growth of a leading-edge separation bubble has been given by Pearcey in Ref. 1; in this report the overall changes in the flow pattern are somewhat simplified from those considered in Ref. 1 since the separation point is fixed at the sharp leading edge of the biconvex section.

A parameter of considerable interest when separation bubbles are present is the quantity $(p_{TE} - p_{0\cdot05c})/H_0$ which is a measure of the pressure recovery over the upper surface of the aerofoil. Fig. 14 shows that after the bubble has become established, the pressure-recovery factor $(p_{TE} - p_{0\cdot05c})/H_0$ decreases as the chordwise extent of the bubble increases with increasing incidence. At $\alpha \simeq 12$ deg the bubble has extended to the trailing edge and there is no pressure recovery over the upper surface of the aerofoil.

Detailed analysis of the pressure distributions obtained in these experiments are presented in Figs. 15 to 18 inclusive. These figures illustrate the growth of the separation bubble as the incidence is increased at a fixed Mach number: a rapid decrease of the local pressure ratio (p/H_0) occurs when the separation bubble reaches a given chordwise station. From these figures and from other pressure distributions not herewith reproduced, it is possible to determine the variation of bubble length with incidence. Since the reattachment process occurs over a finite chordwise distance it is convenient to define the beginning and end of the reattachment process in some arbitrary manner. Fig. 19 illustrates the definitions used in this paper and shows that the specific term ' bubble length ' is very difficult to define (this is particularly so at high incidences when the bubble is of large chordwise extent).

Figs. 20 and 21 show the beginning and end of the reattachment process as a function of incidence for various Mach numbers. In particular, Fig. 20 shows that the beginning of the

reattachment process is almost unaffected by a Mach-number increase from 0·40 to 0·70 and the corresponding Reynolds-number increase from $1{\cdot}9 \times 10^6$ to $2{\cdot}9 \times 10^6$. These results suggest that the position of transition has little effect on the reattachment process for sharp-nosed aerofoils.

Unlike the beginning of reattachment, the end of the reattachment process is significantly affected by change of Mach number. The curves of Fig. 21 indicate that ' bubble length ' will increase as the free-stream Mach number is raised at constant incidence. This is confirmed by the schlieren photographs which are presented in Fig. 22 for Mach numbers of 0·40, 0·50, 0·60 and 0·70 at incidences of 5 and 9 deg. Also from Fig. 21 it may be noted that the bubble length is 36 per cent chord when $\alpha = 4{\cdot}5$ deg and $M_0 = 0{\cdot}40$ and when $\alpha = 3{\cdot}5$ deg and $M_0 = 0{\cdot}70$: the divergence of trailing-edge pressure is shown to occur under these conditions in Fig. 10.

Some details of the flow over the nose of the aerofoil at $M_0 = 0{\cdot}60$ and 0·70 are given by the direct-shadow photographs of Figs. 23 and 24. Again, the initial shape of the bubble is seen to be relatively unaffected by the change of Mach number from 0·60 to 0·70.

Finally, it may be noted that the bubble pressure coefficient C_{pB}, defined by

$$C_{pB} = \left[\left(\frac{p}{H_0}\right)_B - \left(\frac{p}{H_0}\right)_0\right] \Big/ \frac{\frac{1}{2}\rho_0 V_0^2}{H_0}$$

is approximately -1, independent of incidence; this is in agreement with experiments by McCullough and Gault[5].

4. *Conclusions.*—The development of leading-edge flow separation as incidence is raised, for a 4 per cent thick two-dimensional biconvex aerofoil, has been studied over a range of Mach number from 0·40 to 0·70 and a wide incidence range. Whilst the beginning of the flow-attachment process is independent of Mach number, the end of the reattachment process is significantly altered by Mach-number changes, and the length of the bubble of separated flow increases with increase of Mach number at a fixed incidence.

Acknowledgements.—Mr. P. J. Peggs assisted in the experimental work and Mrs. N. A. North assisted in the data reduction.

NOTATION

M_0		Tunnel free-stream Mach number
p		Local static pressure
c		Aerofoil chord
x		Distance along chord measured from leading edge
H_0		Tunnel stagnation pressure
α		Incidence of aerofoil
C_N		Normal-force coefficient
ρ_0		Free-stream density
V_0		Free-stream velocity
p_0		Free-stream static pressure
C_p	$= (p - p_0)/\frac{1}{2}\rho_0 V_0^2$	Pressure coefficient

Suffices

$_{TE}$	Conditions at trailing edge of aerofoil
$_B$	Conditions applicable to bubble of separated flow
$_{BR}$	Conditions applicable to the beginning of the reattachment process
$_{ER}$	Conditions applicable to the end of the reattachment process

REFERENCES

No.	*Author*	*Title, etc.*
1	H. H. Pearcey	A qualitative discussion on the development of leading-edge flow separation for a 6 per cent thick two-dimensional aerofoil at $M = 0{\cdot}4$. A.R.C. 17,981. November, 1955.
2	H. H. Pearcey	Some effects of shock-induced separation of turbulent boundary layers in transonic flow past aerofoils (Paper No. 9 presented at the Symposium on Boundary Layer Effects in Aerodynamics at N.P.L., 31st March to 2nd April, 1955). A.R.C. 17,681. June, 1955.
3	B. D. Henshall and R. F. Cash ..	The interaction between shock waves and boundary layers at the trailing edge of a double-wedge aerofoil at supersonic speed. R. & M. 3004. March, 1955.
4	G. E. Gadd, D. W. Holder and J. D. Regan.	An experimental investigation of the interaction between shock waves and boundary layers. *Proc. Roy. Soc.* A. Vol. 226. pp. 227 to 253. 1954.
5	G. B. McCullough and D. E. Gault	Examples of three representative types of airfoil-section stall at low speed. N.A.C.A. Tech. Note 2502. September, 1951.

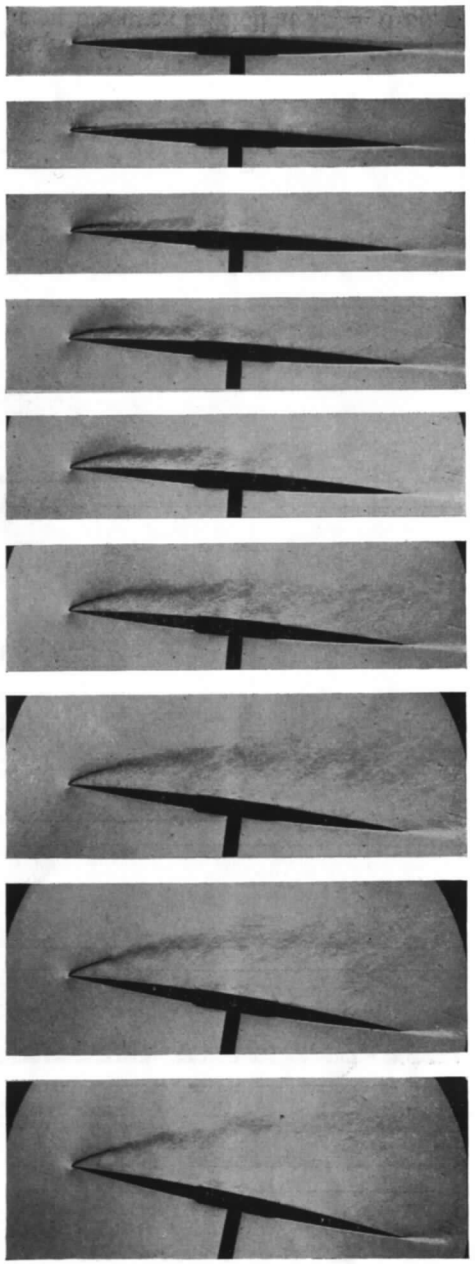

FIG. 1. Schlieren photographs of a 4 per cent biconvex aerofoil at $M_0 = 0{\cdot}40$.

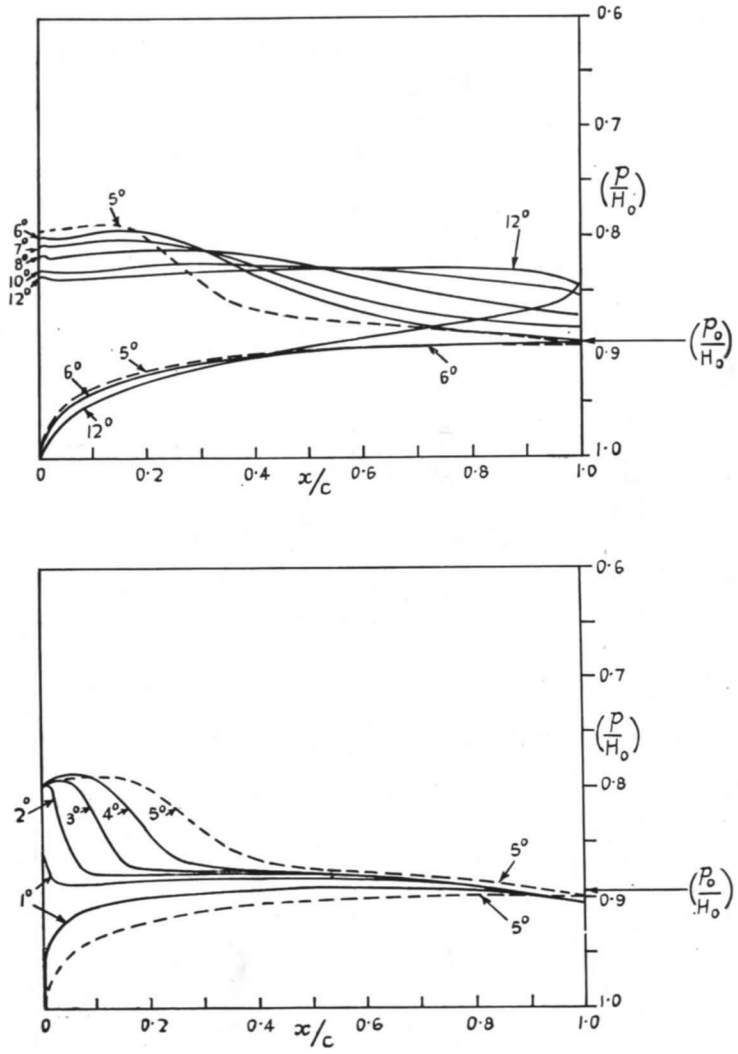

FIG. 2. Surface-pressure distributions for a 4 per cent biconvex aerofoil at $M_0 = 0{\cdot}40$.

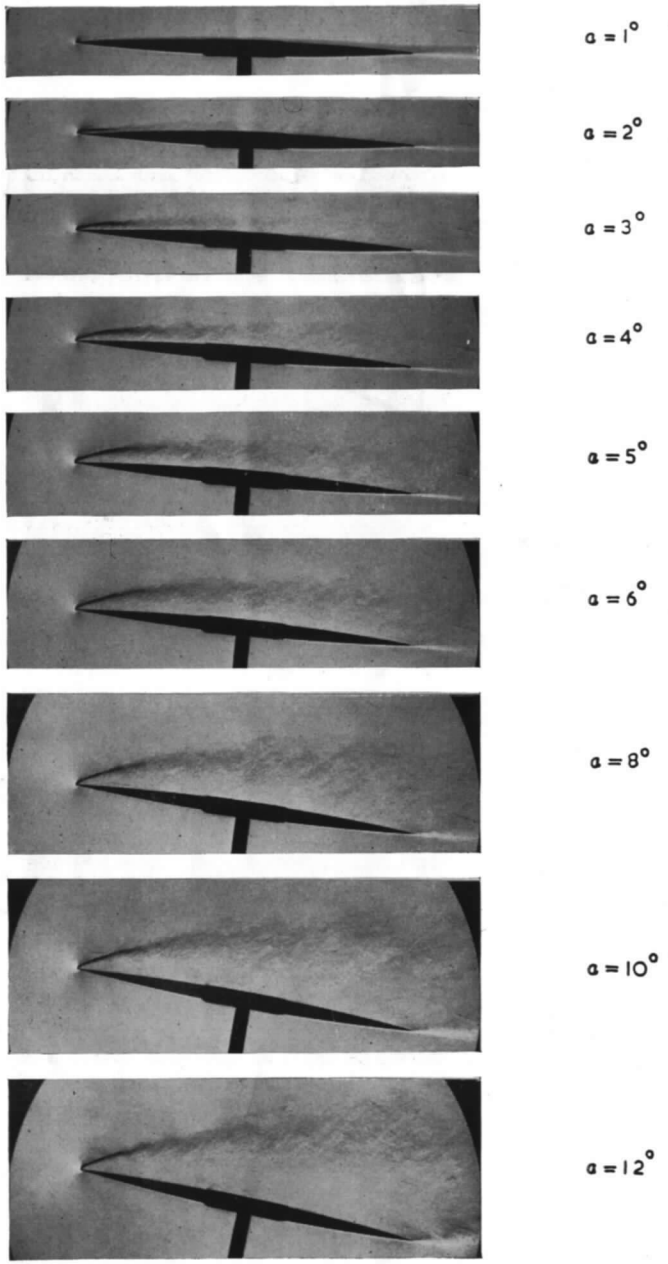

FIG. 3. Schlieren photographs of a 4 per cent biconvex aerofoil at $M_0 = 0{\cdot}50$.

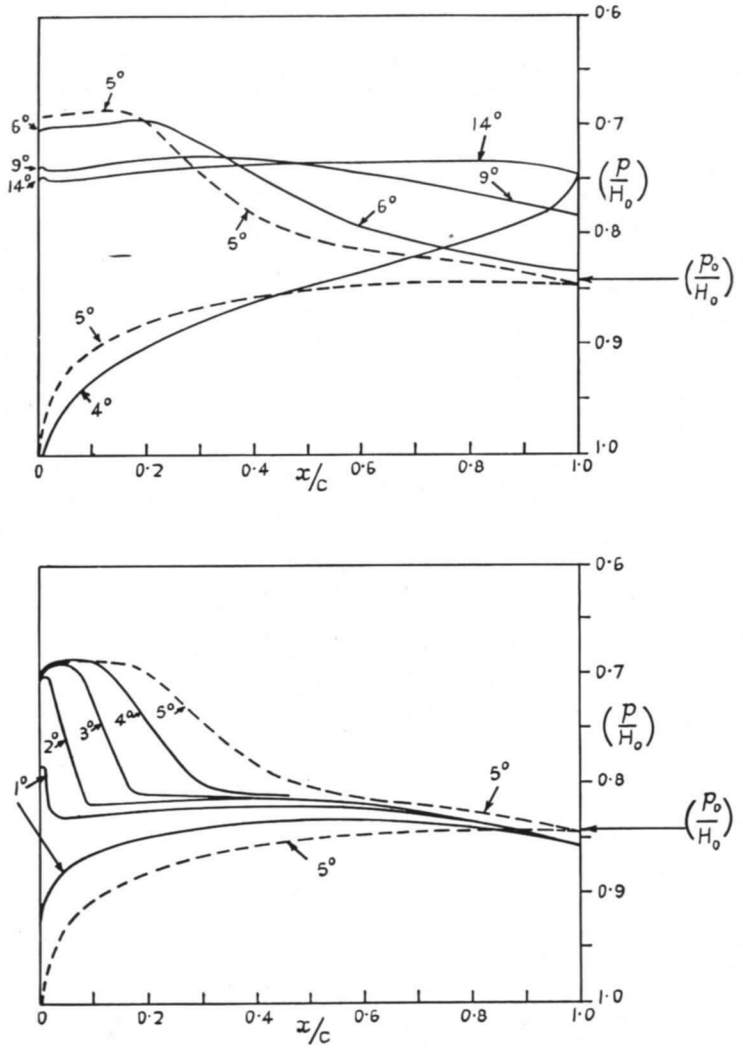

FIG. 4. Surface-pressure distributions for a 4 per cent biconvex aerofoil at $M_0 = 0{\cdot}50$.

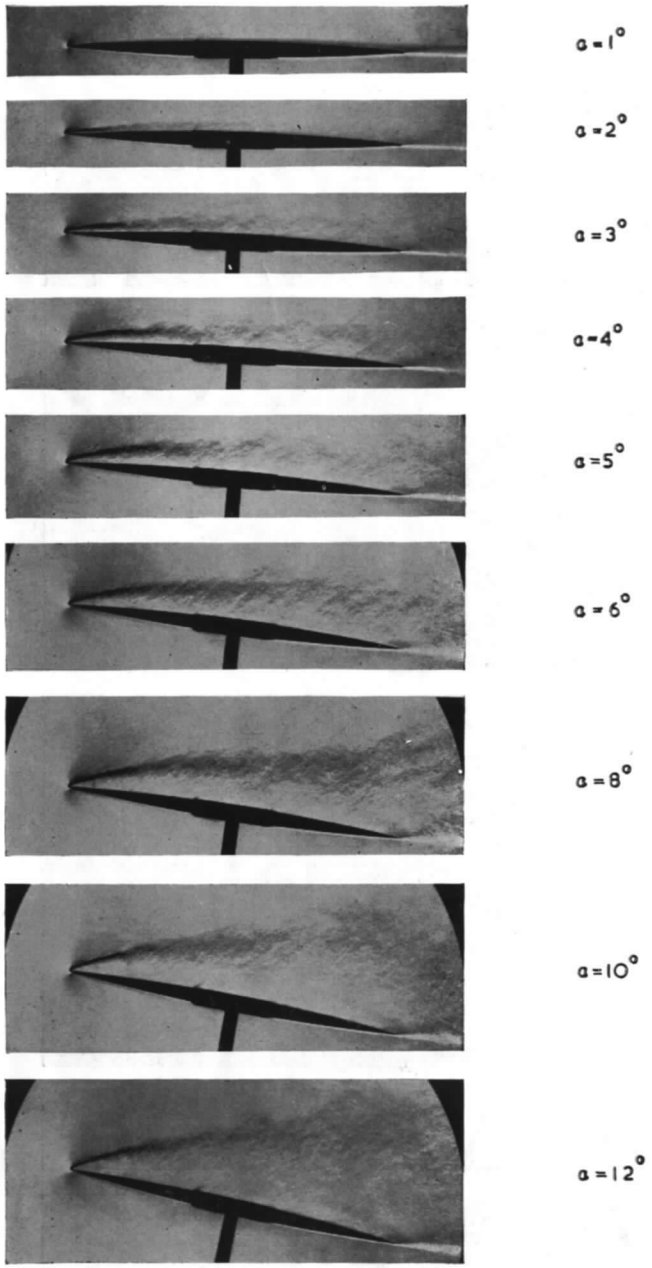

FIG. 5. Schlieren photographs of a 4 per cent biconvex aerofoil at $M_0 = 0{\cdot}60$.

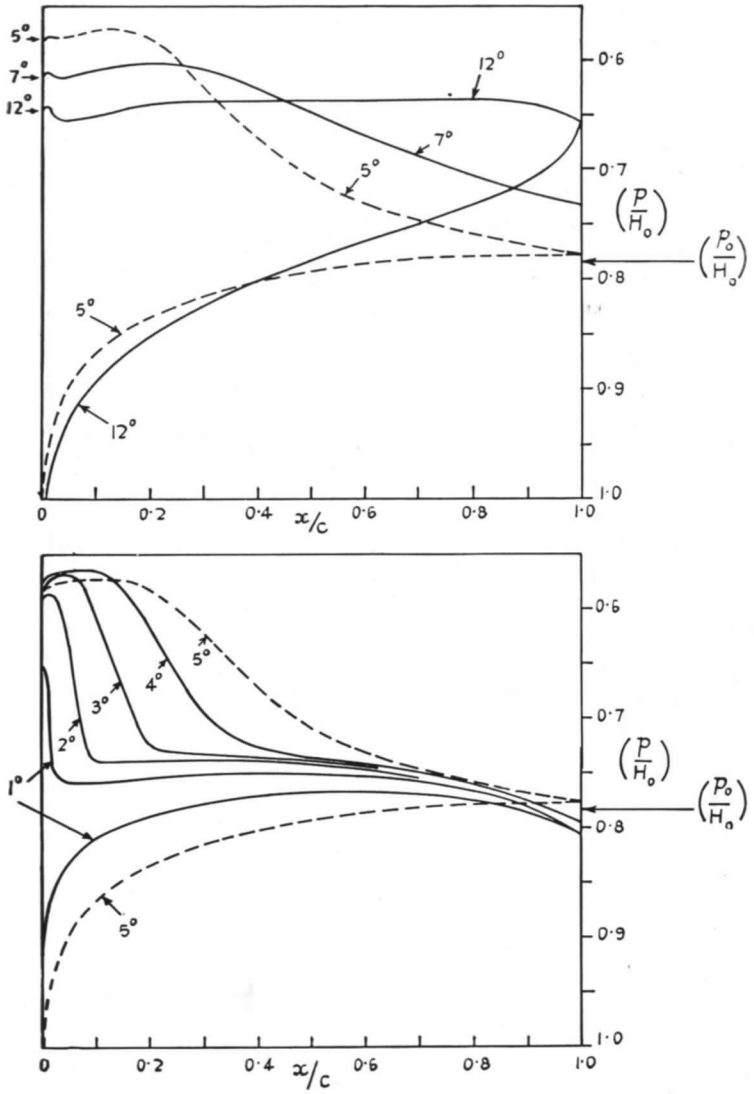

FIG. 6. Surface-pressure distributions for a 4 per cent biconvex aerofoil at $M_0 = 0{\cdot}60$.

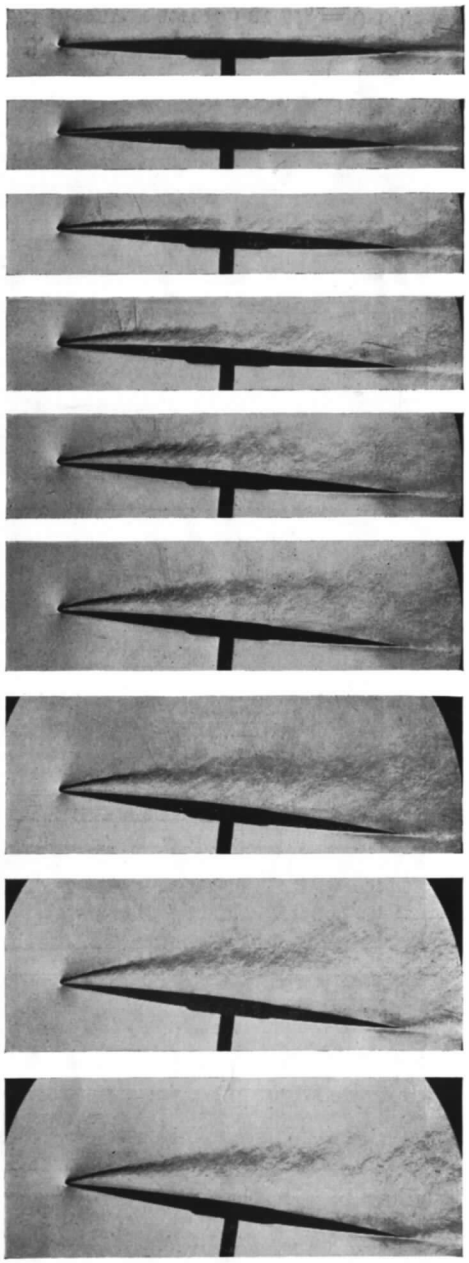

FIG. 7. Schlieren photographs of a 4 per cent biconvex aerofoil at $M_0 = 0{\cdot}70$.

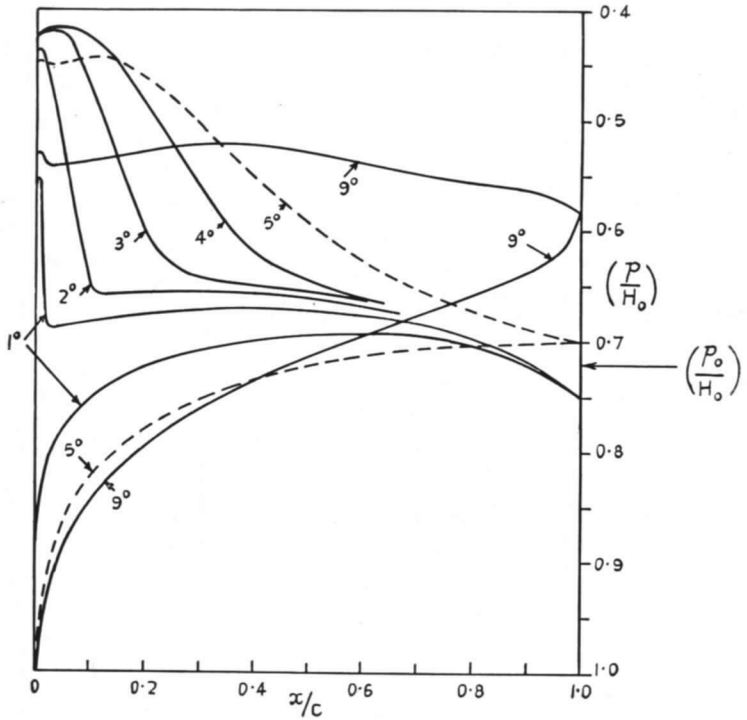

FIG. 8. Surface-pressure distributions for a 4 per cent biconvex aerofoil at $M_0 = 0{\cdot}70$.

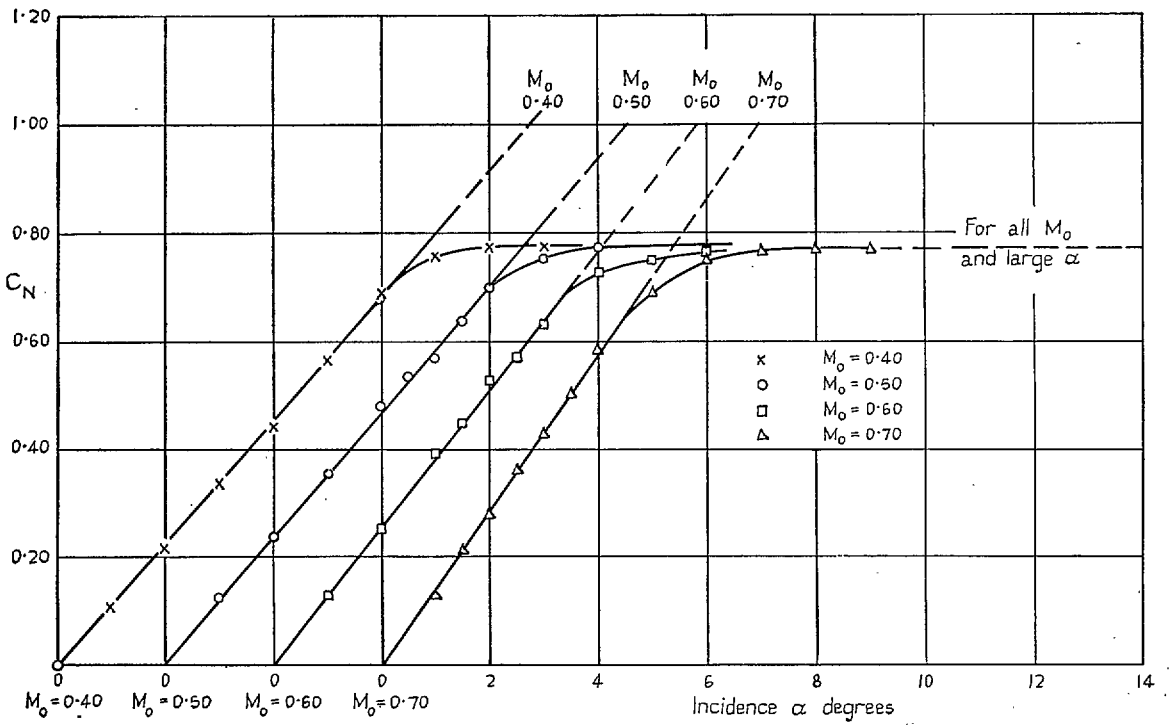

FIG. 9. Variation of normal-force coefficient with incidence for 4 per cent biconvex aerofoil.

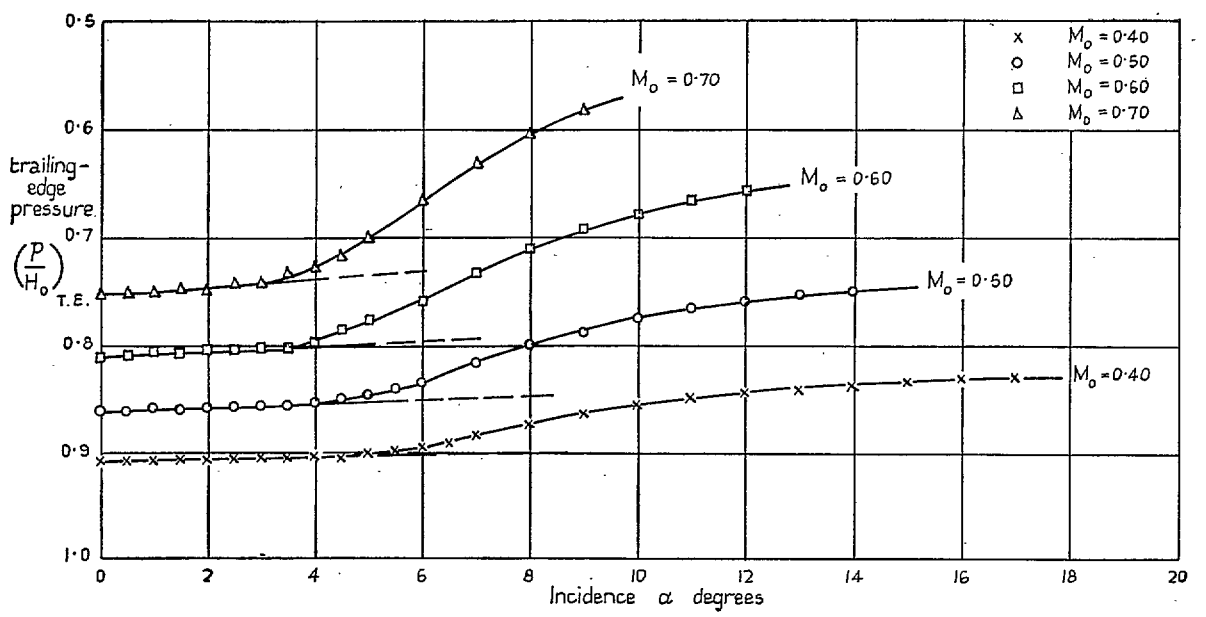

FIG. 10. Variation of trailing-edge pressure with incidence for 4 per cent biconvex aerofoil.

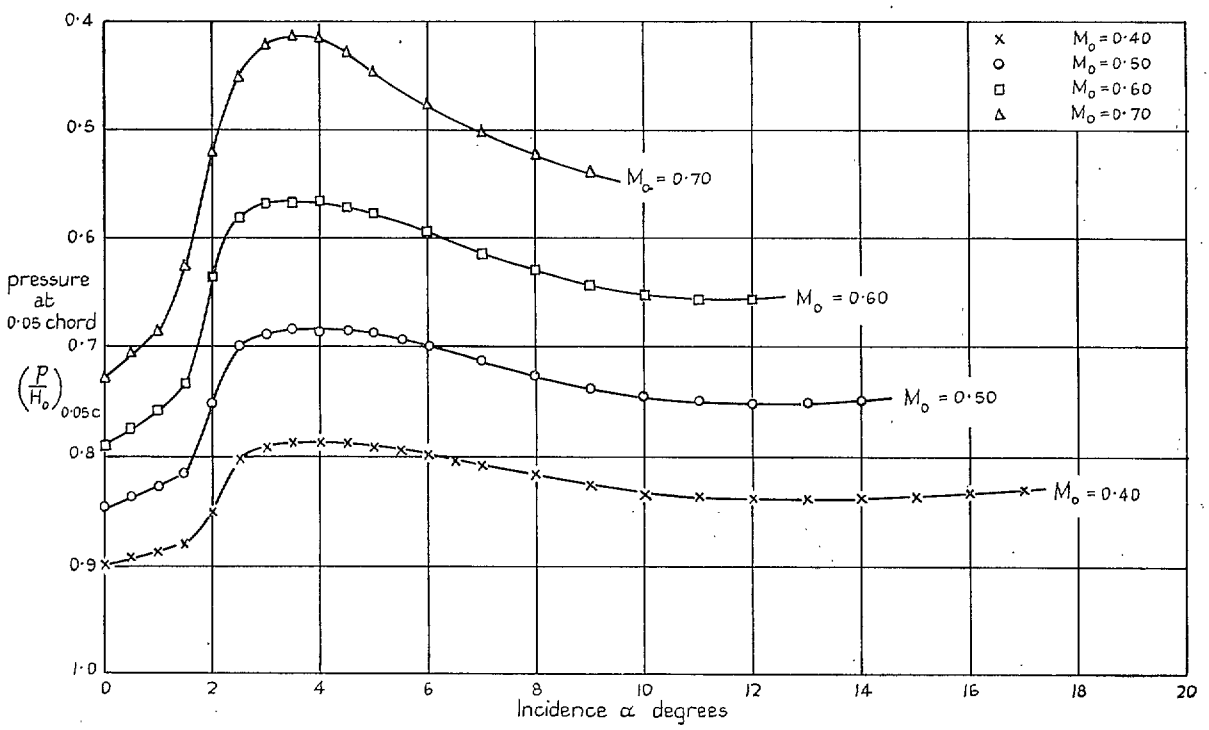

FIG. 11. Variation of pressure at $0\cdot05c$ with incidence for 4 per cent biconvex aerofoil

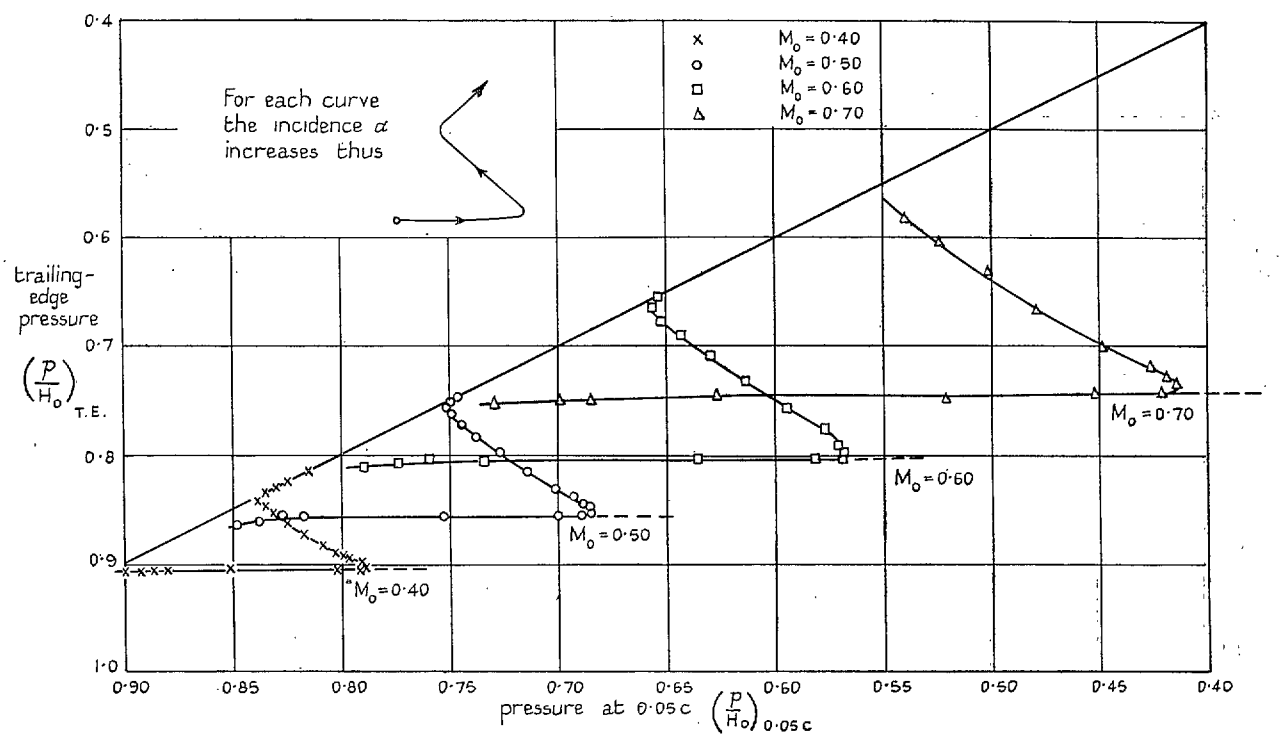

FIG. 12. Variation of pressure at $0\cdot05c$ with trailing-edge pressure for 4 per cent biconvex aerofoil.

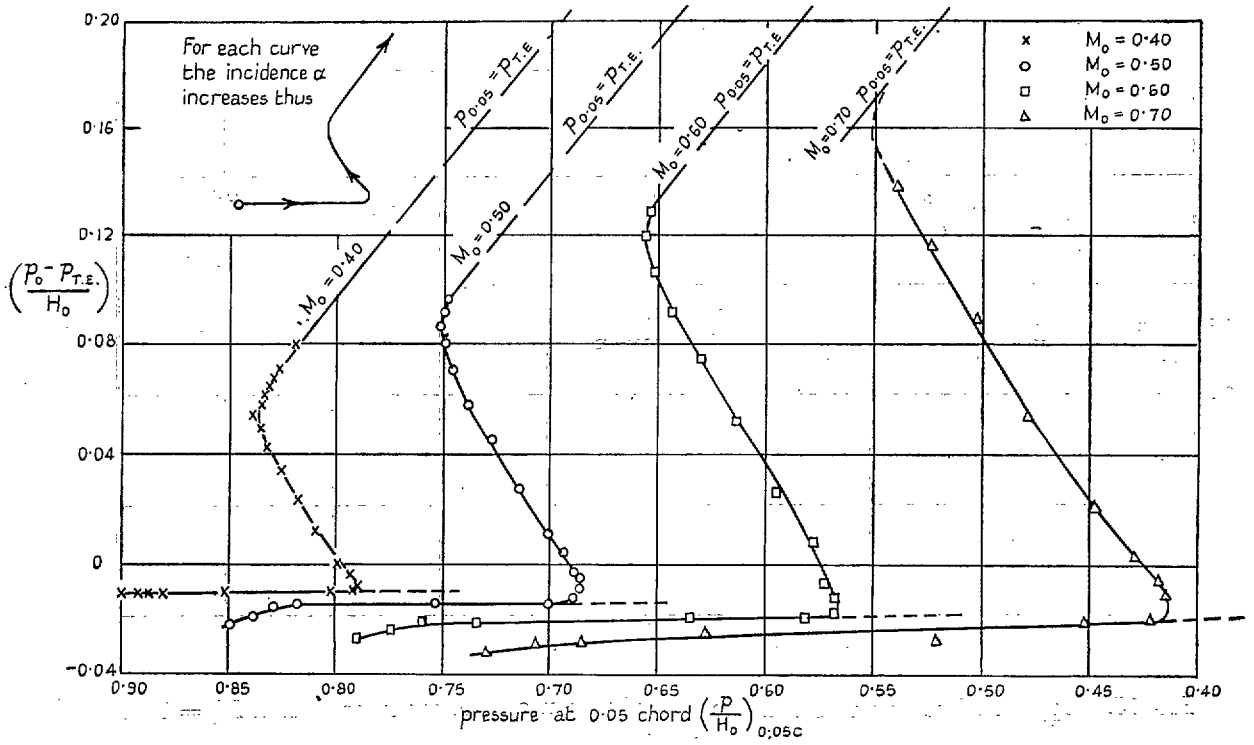

FIG. 13. Variation of pressure at $0{\cdot}05c$ with the factor $(p_0 - p_{TE})/H_0$ for 4 per cent biconvex aerofoil

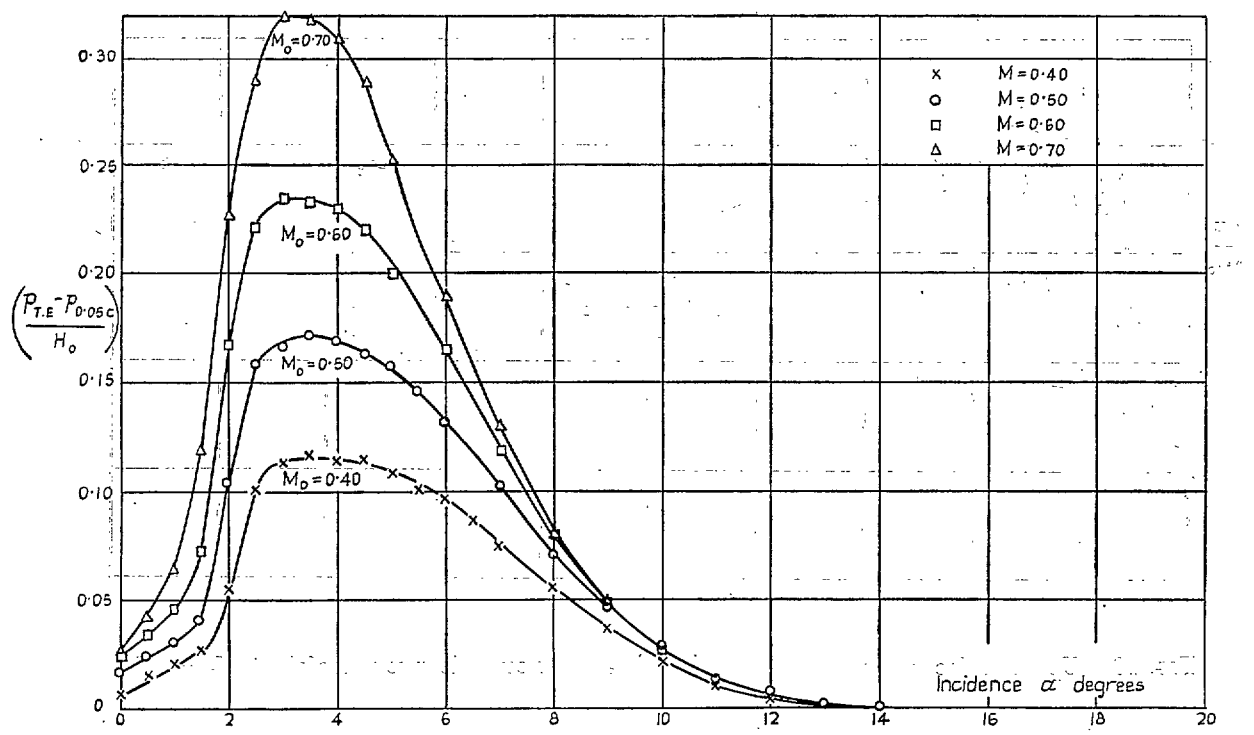

FIG. 14. Variation of quantity $(p_{TE} - p_{0{\cdot}05c})/H_0$ with incidence for 4 per cent biconvex aerofoil.

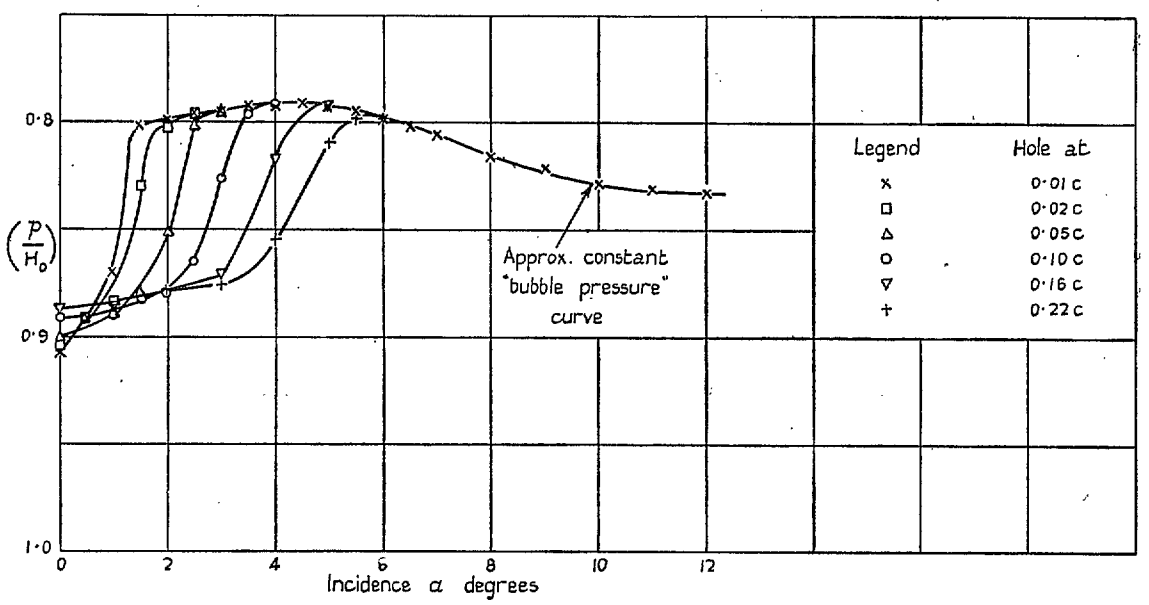

FIG. 15. Upper-surface pressures over the nose of a 4 per cent biconvex aerofoil at $M_0 = 0{\cdot}40$.

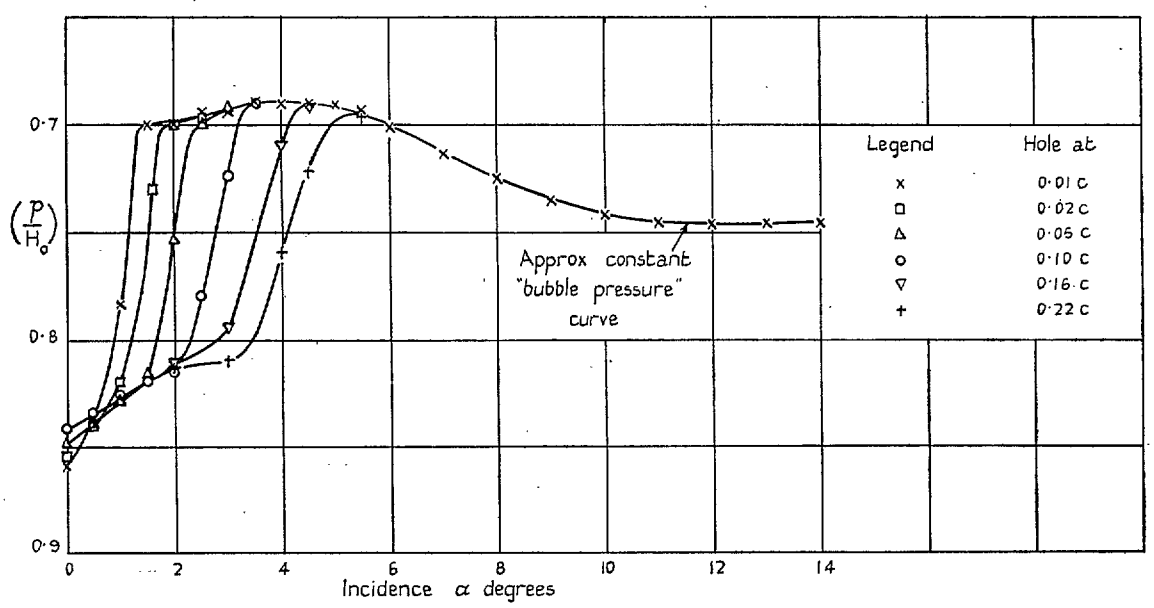

FIG. 16. Upper-surface pressures over the nose of a 4 per cent biconvex aerofoil at $M_0 = 0{\cdot}50$.

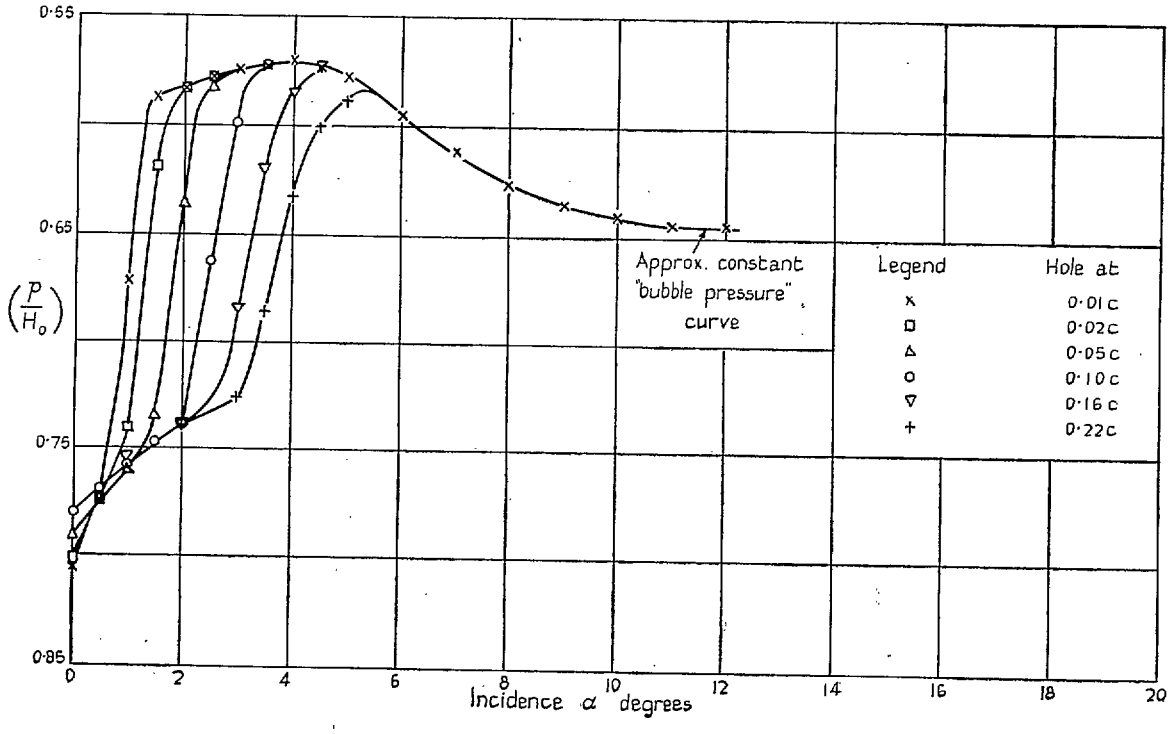

FIG. 17. Upper-surface pressures over the nose of a 4 per cent biconvex aerofoil at $M_0 = 0{\cdot}60$.

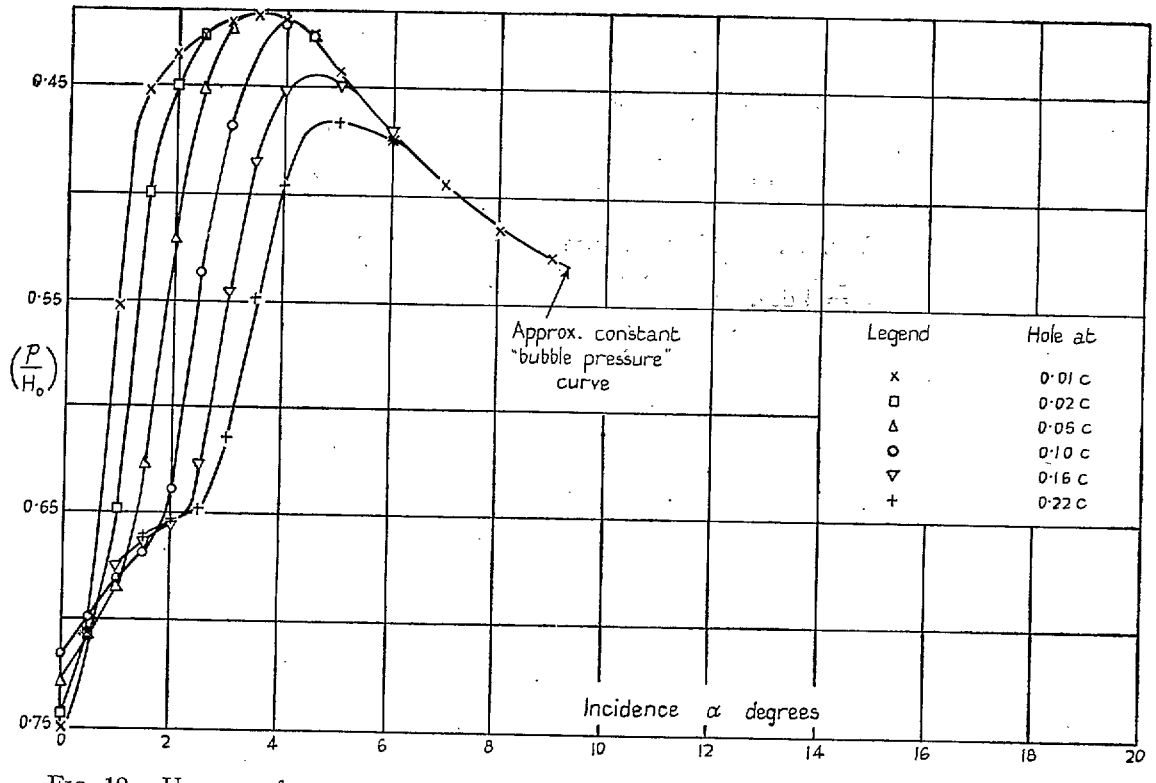

FIG. 18. Upper-surface pressures over the nose of a 4 per cent biconvex aerofoil at $M_0 = 0{\cdot}70$.

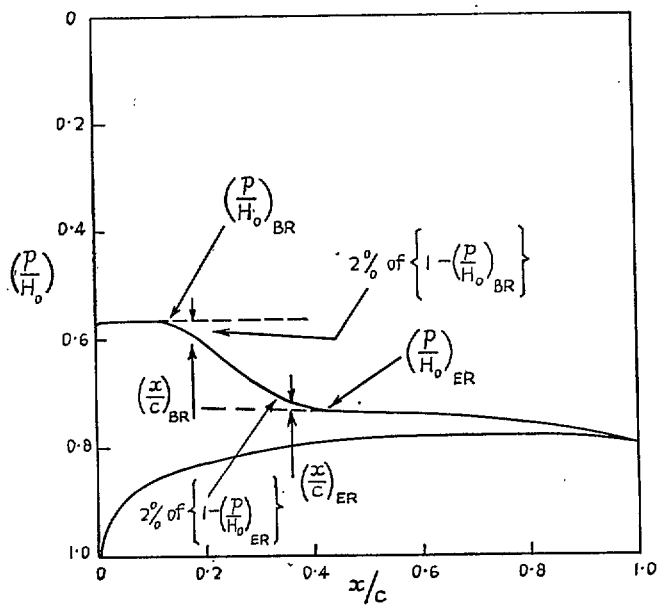

FIG. 19. Surface-pressure distribution for a 4 per cent biconvex aerofoil at $M_0 = 0{\cdot}60$ and $\alpha = 4$ deg, illustrating the beginning and end of the reattachment process.

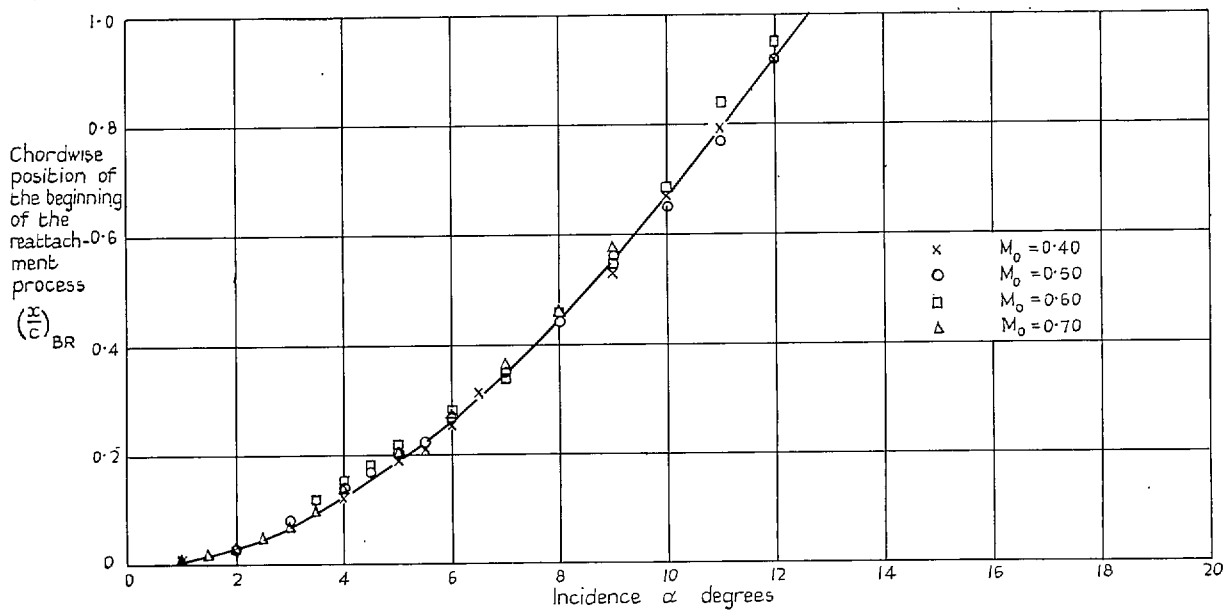

FIG. 20. Variation of the chordwise position of the beginning of the reattachment process with incidence for 4 per cent biconvex aerofoil.

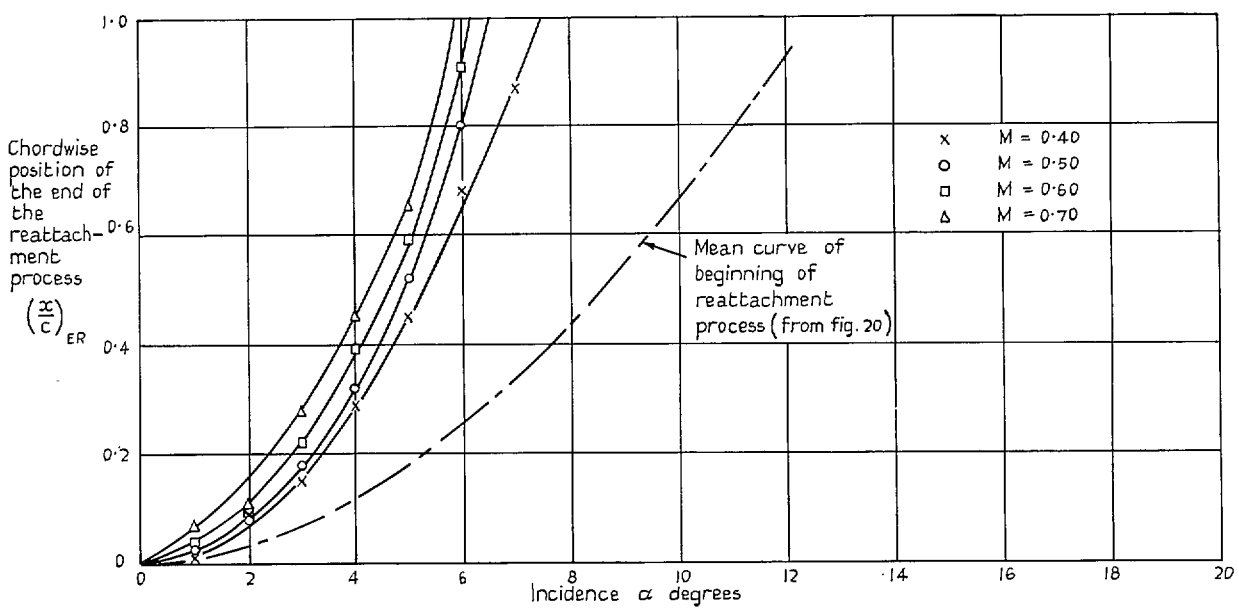

FIG. 21. Variation of the chordwise position of the end of the reattachment process with incidence for 4 per cent biconvex aerofoil.

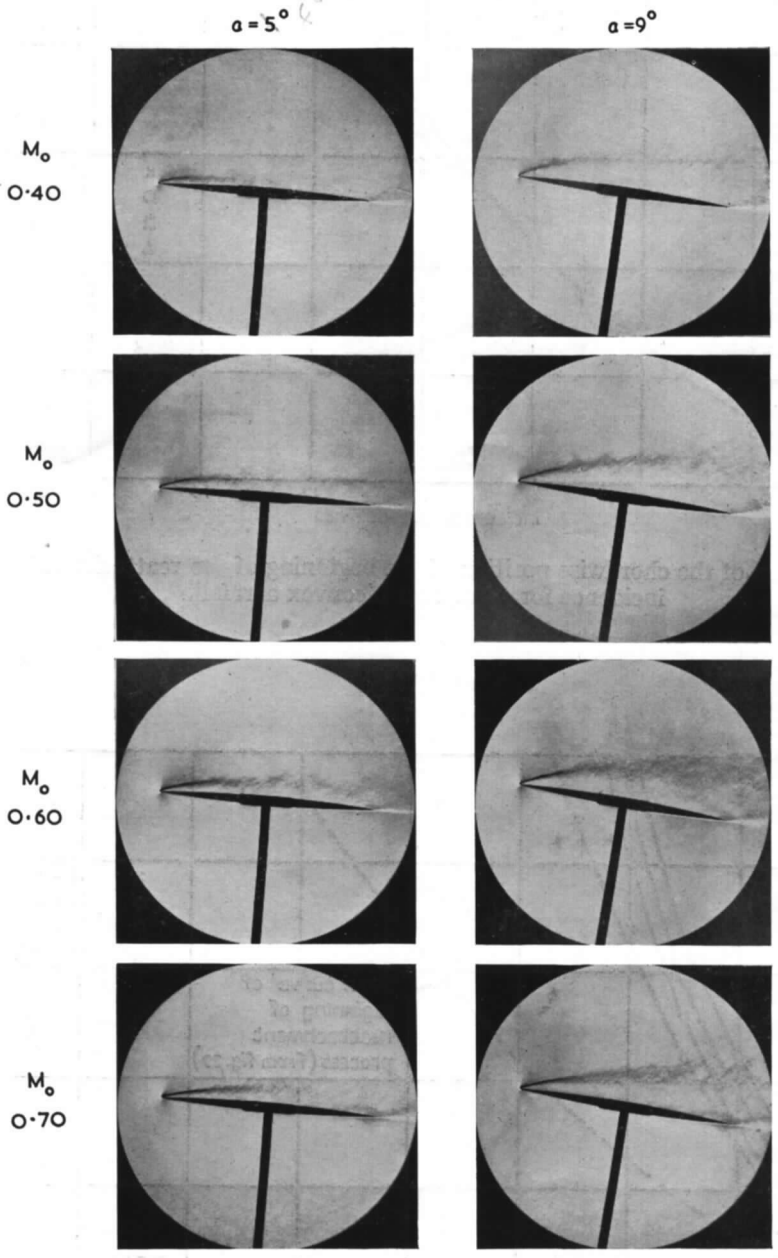

FIG. 22. Schlieren photographs showing the influence of Mach number on the leading-edge flow separation from a 4 per cent biconvex aerofoil.

(73170) Wt. 53/2293 K. 7 8/58 Hw.

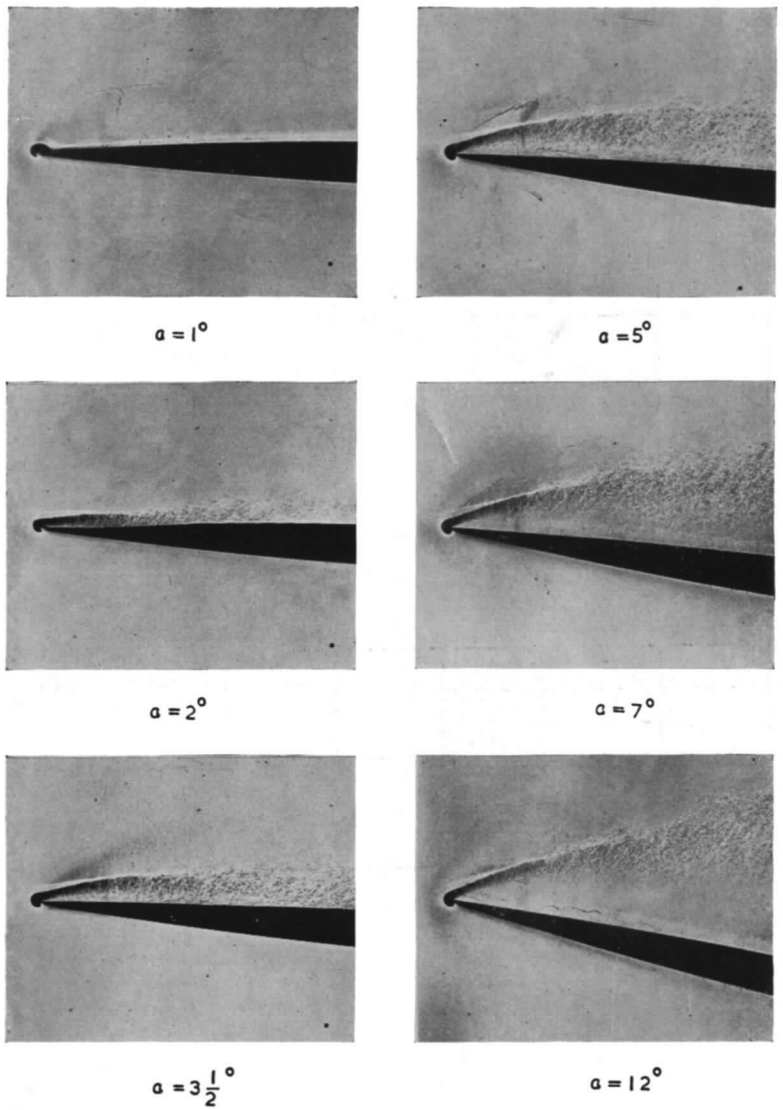

FIG. 23. Direct-shadow photographs of the nose of a 4 per cent biconvex aerofoil at $M_0 = 0{\cdot}60$.

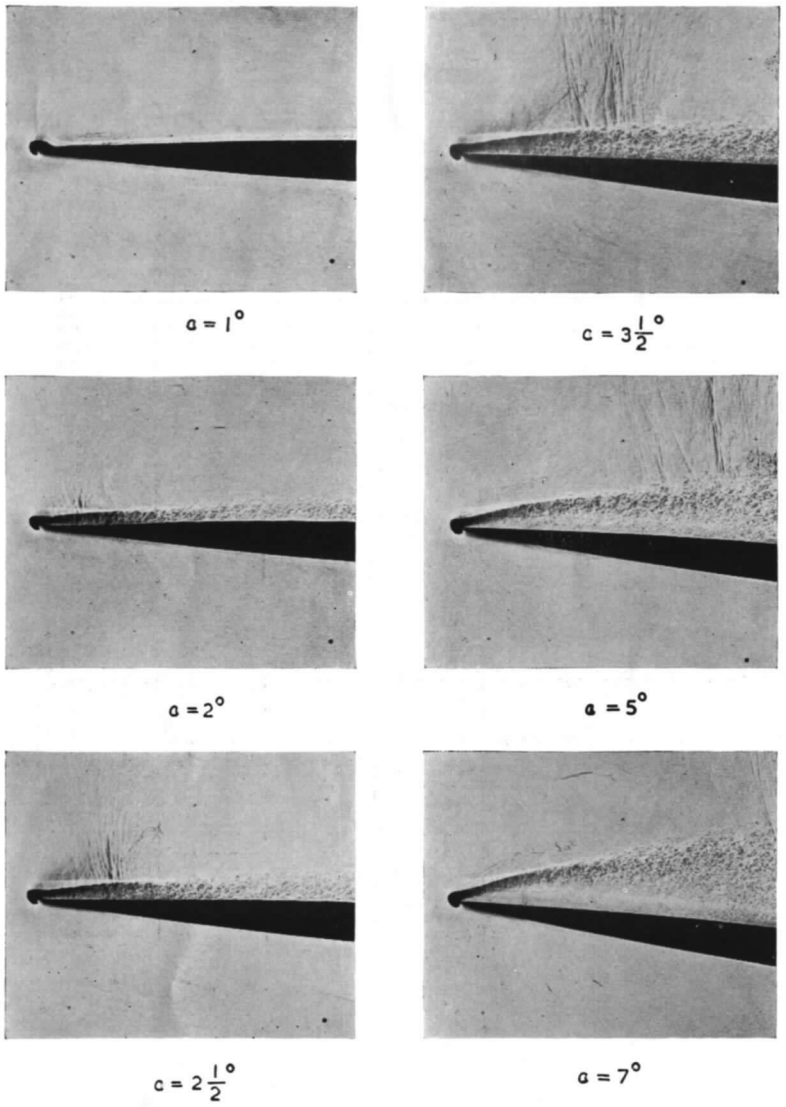

FIG. 24. Direct-shadow photographs of the nose of a 4 per cent biconvex aerofoil at $M_0 = 0{\cdot}70$.

PRINTED IN GREAT BRITAIN

Publications of the Aeronautical Research Council

ANNUAL TECHNICAL REPORTS OF THE AERONAUTICAL RESEARCH COUNCIL (BOUND VOLUMES)

1939 Vol. I. Aerodynamics General, Performance, Airscrews, Engines. 50*s.* (52*s.*).
Vol. II. Stability and Control, Flutter and Vibration, Instruments, Structures, Seaplanes, etc. 63*s.* (65*s.*)

1940 Aero and Hydrodynamics, Aerofoils, Airscrews, Engines, Flutter, Icing, Stability and Control, Structures, and a miscellaneous section. 50*s.* (52*s.*)

1941 Aero and Hydrodynamics, Aerofoils, Airscrews, Engines, Flutter, Stability and Control, Structures. 63*s.* (65*s.*)

1942 Vol. I. Aero and Hydrodynamics, Aerofoils, Airscrews, Engines. 75*s.* (77*s.*)
Vol. II. Noise, Parachutes, Stability and Control, Structures, Vibration, Wind Tunnels. 47*s.* 6*d.* (49*s.* 6*d.*)

1943 Vol. I. Aerodynamics, Aerofoils, Airscrews. 80*s.* (82*s.*)
Vol. II. Engines, Flutter, Materials, Parachutes, Performance, Stability and Control, Structures. 90*s.* (92*s.* 9*d.*)

1944 Vol. I. Aero and Hydrodynamics, Aerofoils, Aircraft, Airscrews, Controls. 84*s.* (86*s.* 6*d.*)
Vol. II. Flutter and Vibration, Materials, Miscellaneous, Navigation, Parachutes, Performance, Plates and Panels, Stability, Structures, Test Equipment, Wind Tunnels. 84*s.* (86*s.* 6*d.*)

1945 Vol. I. Aero and Hydrodynamics, Aerofoils. 130*s.* (132*s.* 9*d.*)
Vol. II. Aircraft, Airscrews, Controls. 130*s.* (132*s.* 9*d.*)
Vol. III. Flutter and Vibration, Instruments, Miscellaneous, Parachutes, Plates and Panels, Propulsion. 130*s.* (132*s.* 6*d.*)
Vol. IV. Stability, Structures, Wind Tunnels, Wind Tunnel Technique. 130*s.* (132*s.* 6*d.*)

Annual Reports of the Aeronautical Research Council—

1937 2*s.* (2*s.* 2*d.*) 1938 1*s.* 6*d.* (1*s.* 8*d.*) 1939–48 3*s.* (3*s.* 5*d.*)

Index to all Reports and Memoranda published in the Annual Technical Reports, and separately—

April, 1950 - - - - R. & M. 2600 2*s.* 6*d.* (2*s.* 10*d.*)

Author Index to all Reports and Memoranda of the Aeronautical Research Council—

1909—January, 1954 R. & M. No. 2570 15*s.* (15*s.* 8*d.*)

Indexes to the Technical Reports of the Aeronautical Research Council—

December 1, 1936—June 30, 1939	R. & M. No. 1850	1*s.* 3*d.* (1*s.* 5*d.*)
July 1, 1939—June 30, 1945	R. & M. No. 1950	1*s.* (1*s.* 2*d.*)
July 1, 1945—June 30, 1946	R. & M. No. 2050	1*s.* (1*s.* 2*d.*)
July 1, 1946—December 31, 1946	R. & M. No. 2150	1*s.* 3*d.* (1*s.* 5*d.*)
January 1, 1947—June 30, 1947	R. & M. No. 2250	1*s.* 3*d.* (1*s.* 5*d.*)

Published Reports and Memoranda of the Aeronautical Research Council—

Between Nos. 2251–2349	R. & M. No. 2350	1*s.* 9*d.* (1*s.* 11*d.*)
Between Nos. 2351–2449	R. & M. No. 2450	2*s.* (2*s.* 2*d.*)
Between Nos. 2451–2549	R. & M. No. 2550	2*s.* 6*d.* (2*s.* 10*d.*)
Between Nos. 2551–2649	R. & M. No. 2650	2*s.* 6*d.* (2*s.* 10*d.*)
Between Nos. 2651–2749	R. & M. No. 2750	2*s.* 6*d.* (2*s.* 10*d.*)

Prices in brackets include postage

HER MAJESTY'S STATIONERY OFFICE

York House, Kingsway, London W.C.2; 423 Oxford Street, London W.1; 13a Castle Street, Edinburgh 2; 39 King Street, Manchester 2; 2 Edmund Street, Birmingham 3; 109 St. Mary Street, Cardiff; Tower Lane, Bristol 1; 80 Chichester Street, Belfast, *or through any bookseller.*

S.O. Code No. 23-3091